CERN-TH/2001-036
April 2002

Pair production of charged Higgs scalars from electroweak gauge boson fusion

S. Moretti

Theory Division, CERN, CH-1211 Geneva 23, Switzerland

Abstract

We compute the contribution to charged Higgs boson pair production at the Large Hadron Collider (LHC) due to the scattering of two electroweak (EW) gauge bosons, these being in turn generated via bremsstrahlung off incoming quarks: $qq \to qqV^*V^* \to qqH^+H^-$ ($V = \gamma, Z, W^\pm$). We verify that the production cross section of this mode is $\tan\beta$ independent and show that it is smaller than that of H^+H^- production via qq-initiated processes but generally larger than that of the loop-induced channel $gg \to H^+H^-$. Pair production of charged Higgs bosons is crucial in order to test EW symmetry breaking scenarios beyond the Standard Model (SM). We show that the detection of these kind of processes at the standard LHC is however problematic, because of their poor production rates and the large backgrounds.

1 Introduction

A charged scalar state does not belong to the particle spectrum of the SM. Therefore, to detect a signal of it would definitely confirm the existence of New Physics. A framework that can naturally accommodate such a particle is the Minimal Supersymmetric Standard Model (MSSM). This is a realisation of a general two Higgs Doublet Model (2HDM) within the theoretical framework provided by Supersymmetry (SUSY). While the SM incorporates only one 'neutral' Higgs boson, ϕ, the MSSM predicts a pair of 'charged' Higgs bosons $H^\pm$ along with three 'neutral' ones, the CP-even H and h and the CP-odd A [1].

It is then not surprising the considerable interest, that has revived lately [2, 3], in accessing the Higgs sector of the MSSM at the future CERN collider through the detection of charged Higgs boson states. In fact, one may well conjecture that, even in presence of a clear signal of a neutral Higgs particle, it could be difficult to distinguish between the SM and the lightest MSSM Higgs boson. For example, in the so-called 'decoupling regime' of the MSSM, one has that the h couplings to ordinary matter become similar to those of the SM ϕ and, besides, the MSSM Higgs masses are such that $M_h \ll M_H \approx M_A \approx M_{H^\pm}$. In fact, such a decoupling scenario occurs for $M_{H^\pm} \gtrsim 150 - 200$ GeV, for any value of $\tan\beta$[1]. Under these circumstances, it would probably be equally challenging to detect a second neutral Higgs signal, as it would be to select a charged Higgs boson signature. This scenario, though not to be expected necessarily, may be viewed as not at all unreasonable, especially taking into account the latest LEP2 results on the possible existence of a neutral Higgs state with mass of about 110–115 GeV [4] (M_h in the MSSM), which, using the MSSM Higgs mass relations (now, known at two-loops [5]), implies an indirect lower bound on $M_{H^\pm}$ already at 140 GeV in the low $\tan\beta$ region, say, around 3 or so[2].

At the LHC, light charged Higgs scalars (i.e., with $M_{H^\pm} < m_t$) can be produced either in top decays, $t \to bH^+$ (with the top quarks being mainly produced via $gg \to t\bar{t}$), or in pair from quark-antiquark annihilations, $q\bar{q} \to H^+H^-$ [6][3]. Heavy charged Higgs bosons (i.e., with $M_{H^\pm} > m_t$ – those beyond the reach of the Tevatron) are mainly generated via the reaction $g\bar{b} \to \bar{t}H^+$ [9]. (In fact, the two processes, $gg \to t\bar{t}$, with $t \to bH^+$, and $g\bar{b} \to \bar{t}H^+$, can be connected [10, 11] by looking at the generic subprocess $gg \to \bar{t}bH^+$ [12].)

[1]Here, $\tan\beta$ denotes the ratio of the vacuum expectation values of the two Higgs doublets of the MSSM and can conveniently be used to parametrise at tree level the entire Higgs sector, alongside one of the masses, e.g., $M_{H^\pm}$ itself.

[2]The direct experimental limit obtained at LEP2 on $M_{H^\pm}$, based on searches for $e^+e^- \to H^+H^-$ events, is at present much smaller: just below $M_{W^\pm}$ [4].

[3]At the forthcoming Run II of the upgraded Fermilab Tevatron, the first of these channels will allow experimenters to scan the $[M_{H^\pm}, \tan\beta]$ plane for large and small values of $\tan\beta$, say, below 2 and above m_t/m_b, roughly up to the kinematical limit of the $t \to bH^+$ decay, $M_{H^\pm} \approx m_t - m_b$ [7], whereas the second channel will be useful in the intermediate $\tan\beta$ region [8], provided charged Higgs bosons are light enough, as simple phase space suppression severely handicaps pair production at $\sqrt{s} = 2$ TeV.

Alternative production channels at the LHC are, for heavy $M_{H^\pm}$: the $bq \to bH^\pm q'$ mode of Ref. [13]; again, charged Higgs boson pair production, but now supplemented by the loop-induced subprocesses $gg \to H^+H^-$ [14]–[16]; associated production $gg, b\bar{b} \to W^\pm H^\mp$ [17] and $q\bar{q}' \to \Phi H^\pm$, with $\Phi = h, H$ and A [6].

If one makes the assumption that the typical mass scale of sparticle states is much higher than $M_{H^\pm}$ (e.g., $M_{\rm SUSY} = 1$ TeV – as we do throughout the paper), thus preventing the decay of charged Higgs bosons via SUSY channels, the decay signature of $H^\pm$ bosons is fairly model independent and dominated by four decay channels at most [18]: $H^+ \to t\bar{b}$, $H^+ \to \tau^+\nu_\tau$, $H^+ \to c\bar{s}$ and $H^+ \to W^+h$. By exploiting the above production channels in conjunction with these decay modes, it has been shown that $H^\pm$ scalars with masses up to 400 GeV can be discovered at the LHC if $\tan\beta \lesssim 3$ (which is in the neighborhood of the indirect limit from LEP2) or $\tan\beta \gtrsim 10 - 15$ (with the minimum occurring when $M_{H^\pm}$ is close to m_t). Alternatively, if one allows for the contribution of SUSY decay modes, according to Ref. [19], the surviving region $3 \lesssim \tan\beta \lesssim 10$ (with $M_{H^\pm} \lesssim 400$ GeV) should adequately be covered by resorting to the decays $H^\pm \to \tilde{\chi}_1^\pm \tilde{\chi}_1^0$ and $H^\pm \to \tilde{\chi}_1^\pm \tilde{\chi}_2^0, \tilde{\chi}_1^\pm \tilde{\chi}_3^0$, i.e., into combinations of chargino-neutralino pairs[4].

Once charged Higgs bosons will have been detected through the leading production channels, and their mass measured, the emphasis will turn to studying their properties. In fact, with the high luminosity of the LHC, also the various subleading production processes would be established experimentally. Among these, it is the $gg \to H^+H^-$ channel, originally discussed in Ref. [14], that has gathered considerable attention in the recent years [15, 16]. The reason is twofold. Firstly, it in principle allows one to measure directly the strength of the trilinear vertices between charged and neutral CP-even Higgs bosons, hH^+H^- and HH^+H^-, thus shading light on the structure of the Higgs sector of the MSSM[5]. The determination of these couplings is in fact a necessary step in reconstructing the self-interaction terms in the full Higgs potential. In contrast, in all other processes mentioned, only gauge (γH^+H^-, ZH^+H^-, hW^+H^-, HW^+H^- and AW^+H^-) and Yukawa ($t\bar{b}H^-$) couplings can be accessed. Secondly, effects of SUSY could be manifest in the $gg \to H^+H^-$ channel, because of virtual squark loops entering the production stage, even when charged Higgs bosons are too light to decay directly into sparticles. Unfortunately, from these points of views, the $gg \to H^+H^-$ subprocess is biased by the presence of the $q\bar{q} \to H^+H^-$ channel, whose production rates are much larger at the LHC, and a complete phenomenological analysis on how to disentangle the two is still lacking.

[4]According to the typical $H^\pm$ decay rates found in [19], one should not expect the scope of the SM channels to be spoiled by the presence of the new SUSY modes.

[5]As a result of CP-invariance, there exists no AH^+H^- coupling at tree level.

2 Pair production of charged Higgs bosons

The purpose of this paper is to show that, at the LHC, pairs of charged Higgs bosons can also be produced via the fusion of gauge vector bosons, γ, Z and $W^{\pm}$, at rates comparable to those induced by parton fusion in $q\bar{q}$ and gg scatterings. Here, the gauge bosons are emitted by incoming quarks and – to a somewhat lesser extent (because of the proton-proton scattering) – by antiquarks too, and the all process can be sketched as follows:

$$qq \to qqV^*V^* \to qqH^+H^- \qquad (V = \gamma, Z, W^{\pm}), \tag{1}$$

where q refers to both quarks and antiquarks (of any possible flavour) in the appropriate combinations[6]. The Feynman diagrams involved can be found in Fig. 1. However, notice that not all of these appear for each quark flavour combination. (For example, for $u\bar{u} \to u\bar{u}H^+H^-$ no $W^{\pm}$ mediated diagrams enter whereas for $u\bar{u} \to d\bar{d}H^+H^-$ the latter are needed.) Besides, we have not shown the graphs that differ from those depicted in Fig. 1 only in the exchange of a fermion leg, as it happens when identical flavours appear in the initial and final states and we have neglected those in which Higgs bosons are radiated by the quark lines, because of the small Yukawa couplings of the leading valence quarks. The matrix element (ME) of process (1) has been computed by means of helicity amplitude techniques. Furthermore, it has been checked for gauge and BRS invariance and integrated numerically over a four-body phase space.

The total cross section for process (1) at the LHC ($\sqrt{s} = 14$ TeV), before any acceptance cuts, can be found in Fig. 2 (continuous line), compared to the yield of the other two production processes of charged Higgs boson pairs, i.e., $q\bar{q} \to H^+H^-$ and $gg \to H^+H^-$, for three reference values of $\tan\beta$ and with $M_{H^{\pm}}$ in the range 130 to 400 GeV[7]. Notice that in order to obtain a finite answer for process (1) (in the case of photon exchange), we have adopted a non-zero value for the mass of all quark flavours. We have chosen $m_u = m_d = 0.32$ GeV, $m_s = 0.50$ GeV, $m_c = 1.55$ GeV and $m_b = 4.25$ GeV. As for the mass and couplings of the neutral Higgs bosons, we have used the Renormalisation Group (RG) improved one-loop relations of Ref. [21]. (Notice that mixing effects are here irrelevant, i.e., non-zero values of the soft SUSY parameters μ, A_b and A_t entering the definition of Higgs masses and couplings mainly affect the neutral Higgs sector while having negligible impact on the phenomenology of pair production of 'heavy' charged Higgs bosons at the LHC).

Contrary to the $q\bar{q} \to H^+H^-$ and $gg \to H^+H^-$ channels, process (1) shows no visible $\tan\beta$ dependence, because of the tiny contribution of the H, h and A mediated graphs (numbers 15,16 and 18 in Fig. 1). In the first process, such a dependence is induced mainly

[6]For simplicity, we have taken the Cabibbo-Kobayashi-Maskawa mixing matrix to be diagonal.

[7]For reference, hereafter, we use the MRS(LO05A) [20] Parton Distribution Functions (PDFs), with factorisation/renormalisation scale $Q = \mu = \sqrt{\hat{s}}$, i.e., the centre-of-mass (CM) energy at parton level. Other choices, such as $Q = \mu = p_T^{H^+H^-}$, yield differences of the order of a few percent.

by $b\bar{b} \to H^+H^-$ scatterings, whereas in the second one, it enters via both the triangle and the box quark-graphs: see Fig. 1 of Ref. [16][8]. The overall rate of process (1) is generally larger than that of $gg \to H^+H^-$ (except for very large $\tan\beta$ values) but smaller than that of $q\bar{q} \to H^+H^-$, though asymptotically (i.e., for very large values of $M_{H^\pm}$), $qq \to qqH^+H^-$ approaches $q\bar{q} \to H^+H^-$. For an annual integrated luminosity of 100 inverse femtobarns, something like 1500 to 150 events of the type (1) could be produced per experiment at the LHC, for charged Higgs boson masses ranging from 140 to 400 GeV.

A word of caution should be spent here though, concerning the simulation of the $b\bar{b}$ component of the $q\bar{q} \to H^+H^-$ process. In fact, the use of a 'phenomenological' b-quark parton density, as available in most PDF sets currently on the market, requires crude approximations of the partonic kinematics, which result in a mis-estimation of the production cross section. (The problem is well known already from the study of the leading production processes of charged Higgs bosons at the LHC, namely, $g\bar{b} \to \bar{t}H^+$ and $gg \to b\bar{t}H^+$: see, e.g., [10, 22].) In practise, the b-(anti)quark in the initial state comes from a gluon in the proton beam splitting into a collinear $b\bar{b}$-pair, resulting in large factors of $\sim \alpha_s \log(Q/m_b)$, where Q is the factorisation scale. These terms are then re-summed to all orders, $\sum_n \alpha_s^n \log^n(Q/m_b)$, in evaluating the phenomenological b-quark PDF. In contrast, in using a gluon density for

$$gg \to b\bar{b}H^+H^- \tag{2}$$

(see Fig. 3 for the associated Feynman graphs), one basically only includes the first terms of the corresponding two series, when the b and $\bar{b}$ in the final state are produced collinearly to the incoming gluon directions. In turns out that, for $Q \gg m_b$, as it is the case here (owing to the presence of two large masses in the final state, so that $Q \gtrsim 2M_{H^\pm}$), the re-summed terms are large and over-compensate the contribution of the large transverse momentum, or p_T, region available in the gluon-induced case. Fig. 4 illustrates this. There, we have plotted the $b\bar{b} \to H^+H^-$ cross section against that for $gg \to b\bar{b}H^+H^-$, for the usual choice PDFs, scales, $\tan\beta$ and $M_{H^\pm}$ values as in the previous plots. For a start, one should appreciate, by comparing Fig. 2 to 4, that $b\bar{b}$ rates are subleading with respect to the $q\bar{q}$ ones, which also include annihilation via u, d, s and c-(anti)quarks, even at very large values of $\tan\beta$, where one might expect the combined effects of the Yukawa couplings entering the $t\bar{b}H^-$ and $b\bar{b}H/h$ vertices to be largest. Moreover, in the heavy mass range, differences between the two cross sections can be even larger than an order of magnitude, well in line with the findings of Refs. [10] and [23], if one considers that two $g \to b\bar{b}$ splittings are involved here. (The sudden rise at $M_{H^\pm} \lesssim m_t - m_b$ seen for the gluon-induced process is due to intermediate top-antitop production, taking place via graphs 1,5,9,10,11,15,16,20,24,25,26,30,31,35 and 39 of Fig. 3.) Despite a well defined procedure exists to combine the $b\bar{b}$- and gg-initiated

[8]Here, for simplicity, we are not including the effects of squark loops in $gg \to H^+H^-$: again, see Fig. 1 of [16]. These can significantly enhance the corresponding cross section, e.g., by up to 50%, depending upon $\tan\beta$, in a Minimal Supergravity (MSUGRA) inspired scenario.

processes, through the subtraction of the common logarithm terms (see [10]), we refrain from doing so here, as Fig. 4 is presented with the sole intention of making clear that current predictions of $b\bar{b}$ contributions to the production of charged Higgs bosons using b-quark densities (see, e.g., some of the results in Ref. [14, 17]) may be too optimistic.

Fig. 5 presents the LHC cross section of the single $H^{\pm}$-production mechanisms discussed above, for $M_{H^{\pm}} \gtrsim m_t$ and our usual three choices of $\tan\beta$. (Here, we have plotted $gg \to \bar{t}bH^+$, accounting for the aforementioned top-antitop production and decay as well as the bg fusion channel, with the mentioned subtraction term included.) Clearly, by comparing Fig. 2 to Fig. 5 (notice the different normalisation), one realises that process (1) is never dominant, although, at $\tan\beta = 7$, it is just above one order of magnitude smaller than the dominant $gg \to \bar{t}bH^+$ mode. The reason of the drop in production rates of the latter process, similarly to what happens for $bq \to bH^{\pm}q'$ and $b\bar{b}, gg \to W^{\pm}H^{\mp}$, see Fig. 5, is due to a coupling of the form

$$\sim \frac{g}{2\sqrt{2}M_{W^{\pm}}} H^+ \left(m_t \cot\beta \bar{t} b_L + m_b \tan\beta \bar{t} b_R\right), \tag{3}$$

whose square – entering the corresponding production cross sections – has a minimum at $\tan\beta \simeq 7$ (this is indeed the reason of the similar trend seen in the previous figures for $b\bar{b} \to H^+H^-$, $gg \to b\bar{b}H^+H^-$ and $gg \to H^+H^-$).

The independence of $\tan\beta$ is an attractive feature that could in principle render process (1) an interesting discovery channel of charged Higgs bosons, complementary to all other modes proportional to the square of the expression in eq. (3)[9]. In fact, a simple measurement of the total cross section $\sigma(qq \to qqH^+H^- \to qqX)$, above the SM rates, would suffice to estimate an $M_{H^{\pm}}$ value, that could then be employed in background suppression in some suitable Higgs decay channel. In order to attempt a Higgs mass reconstruction, we proceed as follows. First, we exploit the presence of two forward/backward jets in the final state of process (1), that can be used for tagging purposes and QCD background suppression, pretty much in the same spirit as in Ref. [24] (see also [25]). There, it was shown how, in the SM Higgs process

$$qq \to qqV^*V^* \to qq\phi \to qqW^+W^-, \tag{4}$$

proceeding via W^+W^- and ZZ fusion ($V = Z, W^{\pm}$), the selection of the two (rather forward/backward) quark-jets in the final state, within a detector acceptance region defined by $p_T^j > 20$ GeV and $|\eta^j| < 5$, can aid to strongly reduce the overwhelming (but rather central) QCD background in $t\bar{t}jj$ and W^+W^-jj events, where j represents a jet, thus rendering process (4) a viable mechanism to detect SM Higgs signals via leptonic W^+W^- decays[10].

[9]The $\tan\beta$ dependence of the $q\bar{q}' \to \Phi H^{\pm}$ processes, with $\Phi = h, H$ and A, is less straightforward than in eq. (3), as all these channels also proceed via $\Phi q\bar{q}$, $\Phi W^{\pm}H^{\mp}$ and $\Phi H^{\pm}H^{\mp}$ vertices, which are more complicated functions of $\tan\beta$, involving in particular the Higgs 'mixing angle' α.

[10]In fact, the decay $W^+W^- \to \ell^+\ell^-\nu_\ell\bar{\nu}_\ell$ represents the best way to extract the SM Higgs signal from the mentioned backgrounds [26, 27] over the mass region between 130 and 180 GeV or so.

The cross section of process (1), after the above transverse momentum and pseudorapidity cuts are enforced, is shown in Fig. 6 (dashed line). The loss of signal events, with respect to the total rate (continuous line), is rather contained (around 35%, typically), owning to the fact that, for $M_{H^\pm} \gtrsim 130-140$ GeV, the bulk of the production rates is due to W^+W^- fusion (followed by ZZ) rather than to $\gamma\gamma$ (or even γZ), which could be relevant only at very small values of $M_{H^\pm}$, as one can deduce from Fig. 7. (Notice the peak at $M_{VV} \approx M_Z$, due to the 'resonant' sub-scattering $W^{+*}W^{-*} \to Z \to H^+H^-$, since we have used $M_{H^\pm} = 10$ GeV as an illustration, value for which the $\gamma\gamma$ contribution is similar in size to the one induced by all the other graphs.) This tendency can already be appreciated by a simple integration over the four-body final state of the two (squared) vector boson propagators in Fig. 1. However, notice that at very low $M_{H^\pm}$ values, despite being numerically stable, the rates for the photon-exchange contributions obtained by using the quark masses as regulators of the otherwise divergent collinear configurations (between initial- and final-state quarks, when the photon is nearly on-shell) are not to be trusted, as these singularities have to be subtracted and absorbed into an additional contribution of the non-perturbative (recall that the masses of u, d and $s-$ quarks are below 1 GeV) photon spectrum inside the proton. Nonetheless we believe that they serve well the purpose of justifying a posteriori our initial calculation of process (1) without any transverse momentum cuts in the forward/backward jets, for the mass region of interest here, $M_{H^\pm} \gtrsim m_t$, where the $\gamma\gamma$ contribution turns out to be negligible. In fact, the final rates presented below for the signal, after our selection procedure, have been obtained in presence of p_T cuts on the various jets, which remove entirely the mentioned singularities.

A tentative selection procedure of the mass resonance in the signal could be the one sketched below. Notice that we carry out our analysis at parton level only, thus neglecting parton shower and hadronisation effects, although we account for typical detector resolutions, as the transverse momenta of all visible particles in the final state have been smeared according to a Gaussian distribution, with $(\sigma(p_T)/p_T)^2 = (0.6/\sqrt{p_T})^2 + (0.04)^2$ for all jets and $(\sigma(p_T)/p_T)^2 = (0.12/\sqrt{p_T})^2 + (0.01)^2$ for the leptons. The missing transverse momentum has been evaluated from the vector sum of the jet and lepton transverse momenta after resolution smearing.

1. We ask for the decays $H^+ \to t\bar{b} \to b\bar{b}W^+$ and $H^- \to \tau^-\bar{\nu}_\tau$, and charge conjugate cases, with the W^+ decaying hadronically to a pair of light jets. At the same time, one requires to tag the τ^- via its leptonic or hadronic decay channels[11]. Hence, the final signature is '6 jets + $\tau^\pm$ + missing energy', with two of the jets being initiated by b-quarks. The largest background to this signature is most probably due to $q\bar{q}, gg \to t\bar{t}gg$ events, with $t \to bW^+$ and $\bar{t} \to \bar{b}\tau^-\bar{\nu}_\tau$, with the two gluons yielding low transverse momentum jets in the forward and backward directions.

[11] We assume that the latter can efficiently be distinguished from the shower of an (anti)quark or gluon.

2. We impose the mentioned transverse momentum and pseudorapidity constraints on all six jets: $p_T^j > 20$ GeV and $|\eta^j| < 5$. Besides, we require that the difference in pseudorapidity between the two quark/gluon-jets with highest and lowest η-value is larger than 2: $|\eta^j_{\rm max} - \eta^j_{\rm min}| \equiv |\eta^{j_1} - \eta^{j_2}| > 2$.

3. Leptons (electrons and/or muons) are accepted if $p_T^\ell > 20$ GeV and $|\eta^\ell| < 2.5$.

4. A pseudorapidity-azimuthal separation between any jet-jet and jet-lepton pair is imposed: $\Delta R \equiv \sqrt{\Delta\eta^2 + \Delta\Phi^2} \geq 0.7$.

5. A threshold on the missing transverse energy is enforced too: $p_T^{\rm miss} > M_{H^\pm}/2$ (here, we make the assumption that the charged Higgs mass is already known).

6. We ask that two quark/gluon-jets (among those not satisfying the last requirement in 1.) reproduce the $W^\pm$ mass within 10 GeV: $|M_{j_3 j_4} - M_{W^\pm}| < 10$ GeV.

7. We further ask that the two above jets reproduce the top mass within 25 GeV, if paired with a third jet: $|M_{j_3 j_4 j_5} - m_t| < 25$ GeV.

8. We impose the veto $|M_{j_6 \tau\nu_\tau} - m_t| > 25$ GeV, where $M_{j_6\tau\nu_\tau}$ is the invariant mass obtained by combining the remaining quark/gluon-jet with the visible τ-momentum and the one of the parent neutrino, the latter being reconstructed by adopting the technique outlined in the fourth paper of [2].

9. We also cut di-jet invariant masses obtained from the two jets already identified in 1. which are below the charged Higgs mass: i.e., $M_{j_1 j_2} > M_{H^\pm}$ (see remark in 5.).

10. Finally, we plot the invariant mass of the four-jet system recoiling against the $j_1 j_2$ and $\tau^\pm$-neutrino pairs.

Although the number of events of type 1. produced via process (1) can still be sizable at the end of the sequence of cuts in 2.–8., and the charged Higgs mass can be reconstructed rather neatly via step 9., see Fig. 8, the background from the QCD events $q\bar{q}, gg \to t\bar{t}gg$ is prohibitive. Despite having been reduced by several orders of magnitude, it overwhelms the Higgs resonances completely. It should in fact be noticed that the integral over the three Higgs curves in Fig. 8, multiplied by the mentioned annual luminosity (i.e., 100 fb^{-1}), yields only 6, 4 and 2 events, in correspondence of $M_{H^\pm} = 215, 310$ and 408 GeV, respectively, whereas the background rates sum up to a total which is typically 1000 times bigger in the vicinity of the peaks. Besides, the above numbers for the $qq \to qqH^+H^-$ process are obtained for $\tan\beta = 40$, value for which the product of the branching ratios of the two channels $H^+ \to t\bar{b} \to b\bar{b}W^+$ and $H^- \to \tau^-\bar{\nu}_\tau$ is maximal, within the theoretically preferred $\tan\beta$ interval, i.e., $\tan\beta \lesssim m_t/m_b$. The situation does not improve substantially for other

values of $M_{H^\pm}$ in the heavy mass range or other, more selective choices of cuts, than those illustrated here.

3 Summary and conclusions

In summary, we have demonstrated that H^+H^- production can be induced at the LHC by three distinct processes: quark-antiquark, vector-vector and gluon-gluon fusion, in order of quantitative importance. Whereas the phenomenological relevance of the first and third of these modes has been recognised for some time (and stressed again recently), that of the second channel constitutes the novelty of our research. Besides, at the LHC, the gg-mode has been advocated as one of the best ways to probe the hH^+H^- and HH^+H^- couplings among Higgs scalars and as an effective means to constrain the squark sector of SUSY, as both neutral Higgs bosons and scalar quarks enter the virtual stages of the production process. Hence, in suppressing the background to $gg \to H^+H^-$, special care has to be adopted in dealing not only with the $q\bar{q} \to H^+H^-$ mode, but also with the $qq \to qqH^+H^-$ channel. Finally, the EW vector-vector fusion reaction has been tested as a possible detection mode of heavy charged Higgs bosons, as a complement to the leading $gg \to \bar{t}bH^+$ channel, the former covering the $3 \lesssim \tan\beta \lesssim 10$ window, where the detection potential of the latter is seriously hampered by a steeply falling production rate (with a minimum at $\tan\beta = 7$). Despite the independence of $qq \to qqH^+H^-$ from $\tan\beta$ could allow for a prompt estimate of $M_{H^\pm}$ and the consequent mass resonance selection can be made viable, the background from QCD induced events of the type $q\bar{q}, gg \to t\bar{t}gg$ is prohibitively large, at least in the channel $H^+H^- \to$ '4 jets + $\tau^\pm$ + missing energy', including the detection of the two quark-jets produced in association with the Higgs boson pair. Consequently, we expect the measurement of the triple Higgs couplings entering process (1) via graphs 15,16 and 18 in Fig. 1 to be extremely difficult. As forward-jet tagging has proved to be a crucial ingredient of our analysis in reducing the QCD noise, and if one also recalls Fig. 2, showing the dominance of $qq \to qqH^+H^-$ over $gg \to H^+H^-$, similar conclusions should apply to the case of the gluon-induced reaction. Finally, even in case signals of the $q\bar{q} \to H^+H^-$ process can be detected (again, see Fig. 2), it should be remembered that sizable effects of Higgs self-couplings enter here only via s-channel $b\bar{b}$-annihilation, which is a small component of the total $q\bar{q}$-induced rate, further considering that the $b\bar{b} \to H^+H^-$ cross section is certainly over-estimated by the current sets of b-quark PDFs, given that the use of the more realistic $gg \to b\bar{b}H^+H^-$ partonic scattering yields a rate which is about an order of magnitude smaller, whenever $M_{H^\pm} \gtrsim m_t$ (recall Fig. 4).

Indeed, if the processes and signature that we have chosen are to be useful in searching for pairs of charged Higgs bosons at the LHC, far better cuts than those designed here will need to be devised. An alternative, cleaner detection mode could be $H^+H^- \to \tau^+\nu_\tau\tau^-\bar{\nu}_\tau$,

however, this requires more realistic simulations (including double $\tau^{\pm}$ reconstruction in a real detector environment) than those that can be carried out in a parton level study. Ultimately, processes of the type $q\bar{q} \to H^+H^-$, $gg \to H^+H^-$ and $qq \to qqH^+H^-$ are primary candidates to benefit from a possible tenfold LHC luminosity upgrade, the so-called SLHC [28], given their rather small production rates at the standard LHC in general.

Acknowledgements

We are grateful to PPARC for financial support and to the Theory Group at the Rutherford Appleton Laboratory (RAL) for hospitality during the early stages of this work. We also thank Kosuke Odagiri for suggesting the topic of this research, for innumerable helpful discussions and for numerical comparisons as well.

References

[1] J.F. Gunion, H.E. Haber, G.L. Kane and S. Dawson, "The Higgs Hunters' Guide" (Addison-Wesley, Reading, MA, 1990).

[2] J.F. Gunion, Phys. Lett. B322 (1994) 125; V. Barger, R.J.N. Phillips and D.P. Roy, Phys. Lett. B324 (1994) 236; S. Raychaudhuri and D.P. Roy, Phys. Rev. D52 (1995) 1556, Phys. Rev. D53 (1996) 4902; K. Odagiri, preprint RAL-TR-1999-012, January 1999, `hep-ph/9901432`, Phys. Lett. B452 (1999) 327; D.P. Roy, Phys. Lett. B459 (1999) 607; S. Moretti and D.P. Roy, Phys. Lett. B470 (1999) 209; M. Drees, M. Guchait and D.P. Roy, Phys. Lett. B471 (1999) 39; D.J. Miller, S. Moretti, D.P. Roy and W.J. Stirling, Phys. Rev. D61 (2000) 055011; S. Moretti, Phys. Lett. B481 (2000) 49; A. Belyaev, D. Garcia, J. Guasch and J. Sola, preprint CERN-TH/2001-051, KA-TP-7-2001, UB-ECM-PF-02/02, FSU-HEP-020301, February 2002, `hep-ph/0203031`.

[3] CMS Technical Proposal, CERN/LHCC/94-38 (1994); ATLAS Technical Proposal, CERN/LHCC/94-43 (1994); K.A. Assamagan, preprint ATL-PHYS-99-013, preprint ATL-PHYS-99-025; K.A. Assamagan and Y. Coadou, preprint ATL-COM-PHYS-2000-017; K.A. Assamagan, A. Djouadi, M. Drees, M. Guchait, R. Kinnunen, J.L. Kneur, D.J. Miller, S. Moretti, K. Odagiri and D.P. Roy, contribution to the Workshop 'Physics at TeV Colliders', Les Houches, France, 8-18 June 1999, preprint PM/00-03, pages 36-53, February 2000, `hep-ph/0002258`; K.A. Assamagan, M. Bisset, Y. Coadou, A.K. Datta, A. Deandrea, A. Djouadi, M. Guchait, Y. Mambrini, F. Moortgat and S. Moretti, contribution to the Workshop 'Physics at TeV Colliders', Les Houches, France, 21 May-1 June 2001, pages 85-110, February 2002, `hep-ph/0203056`.

[4] LEP Higgs Working Group, http://www.cern.ch/LEPHIGGS/.

[5] S. Heinemeyer, W. Hollik and G. Weiglein, Eur. Phys. J. C9 (1999) 343; R.-J. Zhang, Phys. Lett. B447 (1999) 89.

[6] E. Eichten, I. Hinchliffe, K. Lane and C. Quigg, Rev. Mod. Phys. 56 (1984) 579.

[7] See, e.g.: M. Carena, J. Conway, H.E. Haber and J. Hobbs (conveners), 'Report of the Higgs Working Group', Proceedings of the 'Tevatron Run II SUSY/Higgs Workshop', February-November 1998, Fermilab, Batavia, Illinois (unpublished).

[8] K. Odagiri, private communication.

[9] J.F. Gunion, H.E. Haber, F.E. Paige, W.-K. Tung and S.S.D. Willenbrock, Nucl. Phys. B294 (1987) 621.

[10] F. Borzumati, J.-L. Kneur and N. Polonsky, Phys. Rev. D60 (1999) 115011.

[11] M. Guchait and S. Moretti, JHEP 01 (2002) 001.

[12] J.L. Diaz-Cruz and O.A. Sampayo, Phys. Rev. D50 (1994) 6820.

[13] S. Moretti and K. Odagiri, Phys. Rev. D55 (1997) 5627.

[14] S.S.D. Willenbrock, Phys. Rev. D35 (1987) 173.

[15] Y. Jiang, W.-G. Ma, L. Han, M. Han and Z.-H. Yu, J. Phys. G23 (1997) 385, Erratum, ibidem G23 (1997) 1151; A. Krause, T. Plehn, M. Spira and P.M. Zerwas, Nucl. Phys. B519 (1998) 85; A. Belyaev, M. Drees, O.J.P. Eboli, J.K. Mizukoshi and S.F. Novaes, Phys. Rev. D60 (1999) 075008; A. Belyaev, M. Drees and J.K. Mizukoshi, Eur. Phys. J. C17 (2000) 337; A.A. Barrientos Bendezú and B.A. Kniehl, Nucl. Phys. B568 (2000) 305; O. Brein and W. Hollik, Eur. Phys. J. C13 (2000) 175.

[16] Y. Jiang, W.-G. Ma, L. Han, M. Han and Z.-H. Yu, J. Phys. G24 (1998) 83.

[17] D.A. Dicus, J.L. Hewett, C. Kao and T.G. Rizzo, Phys. Rev. D40 (1989) 787; S. Moretti and K. Odagiri, Phys. Rev. D59 (1999) 055008; A.A. Barrientos Bendezú and B.A. Kniehl, Phys. Rev. D59 (1999) 015009, ibidem D61 (2000) 097701, ibidem D63 (2001) 015009; O. Brein, W. Hollik and S. Kanemura, Phys. Rev. D63 (2001) 095001.

[18] S. Moretti and W.J. Stirling, Phys. Lett. B347 (1995) 291, Erratum, ibidem B366 (1996) 451; A. Djouadi, J. Kalinowski and P.M. Zerwas, Z. Phys. C70 (1996) 435; E. Ma, D.P. Roy and J. Wudka, Phys. Rev. Lett. 80 (1998) 1162.

[19] M. Bisset, M. Guchait and S. Moretti, Eur. Phys. J. C19 (2001) 143.

[20] A.D. Martin, R.G. Roberts, W.J. Stirling and R.S. Thorne, Phys. Lett. B443 (1998) 301.

[21] M. Carena, J. Espinosa, M. Quiros and C.E.M. Wagner, Phys. Lett. B355 (1995) 209; H.E. Haber, R. Hempfling and A.H. Hoang, Z. Phys. C75 (1997) 539.

[22] D. Dicus, T. Stelzer, Z. Sullivan and S.S.D. Willenbrock, Phys. Rev. D59 (1999) 094016.

[23] S. Moretti and D.P. Roy, in Ref. [2].

[24] D. Rainwater and D. Zeppenfeld, Phys. Rev. D60 (1999) 113004, Erratum, ibidem D61 (2000) 099901.

[25] T. Plehn, D. Rainwater and D. Zeppenfeld, Phys. Rev. D61 (2000) 093005.

[26] M. Dittmar and H. Dreiner, Phys. Rev. D55 (1997) 167.

[27] S. Moretti, Phys. Rev. D56 (1997) 7427.

[28] F. Gianotti, M.L. Mangano and T. Virdee (conveners), preprint CERN-TH/2002-078, April 2002, `hep-ph/0204087`.

Diagrams by FEYNMAN DRAW

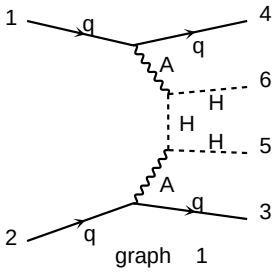

graph 1

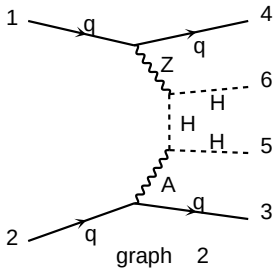

graph 2

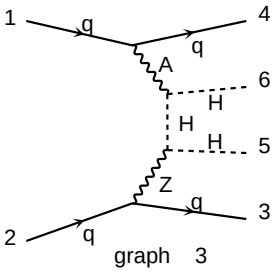

graph 3

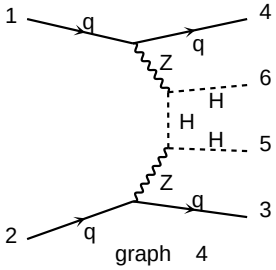

graph 4

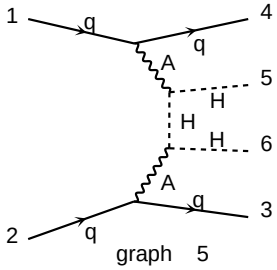

graph 5

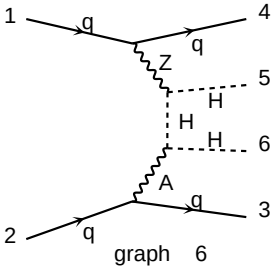

graph 6

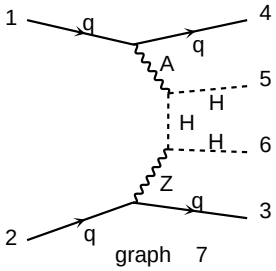

graph 7

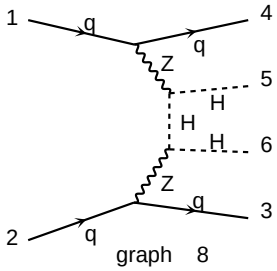

graph 8

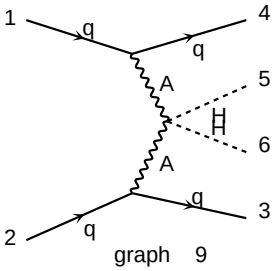

graph 9

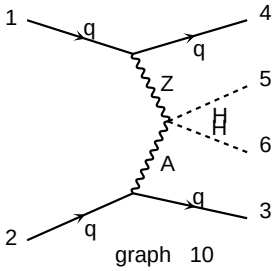

graph 10

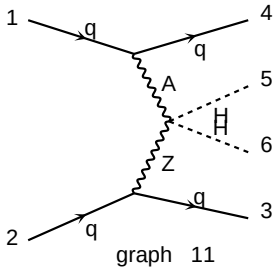

graph 11

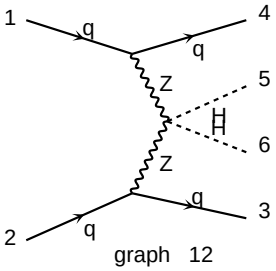

graph 12

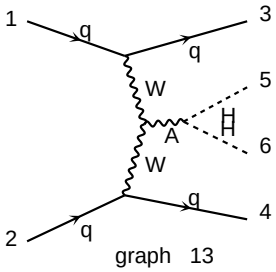

graph 13

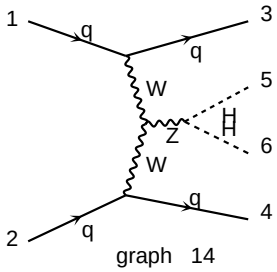

graph 14

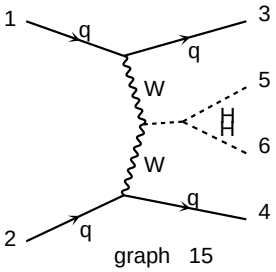

graph 15

continue

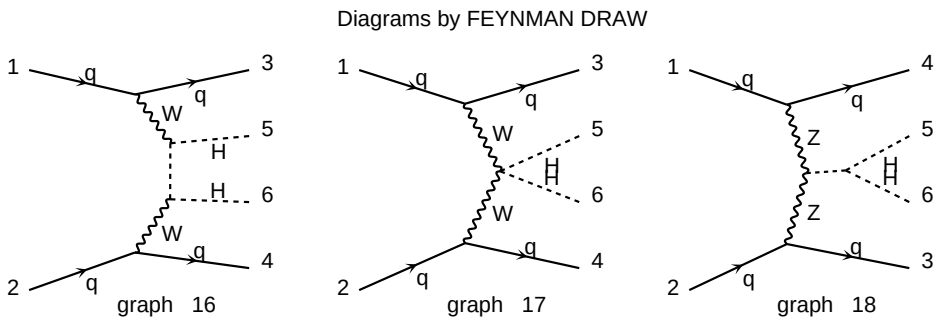

Figure 1: Feynman diagrams at tree level for process (1). The labels `q, A, Z, W and H` refer to a (anti)quark, γ, Z, $W^{\pm}$ and $H^{\pm}$ boson, respectively, whereas an unlabelled, internal dashed line represents a summation over H, h and A boson propagators.

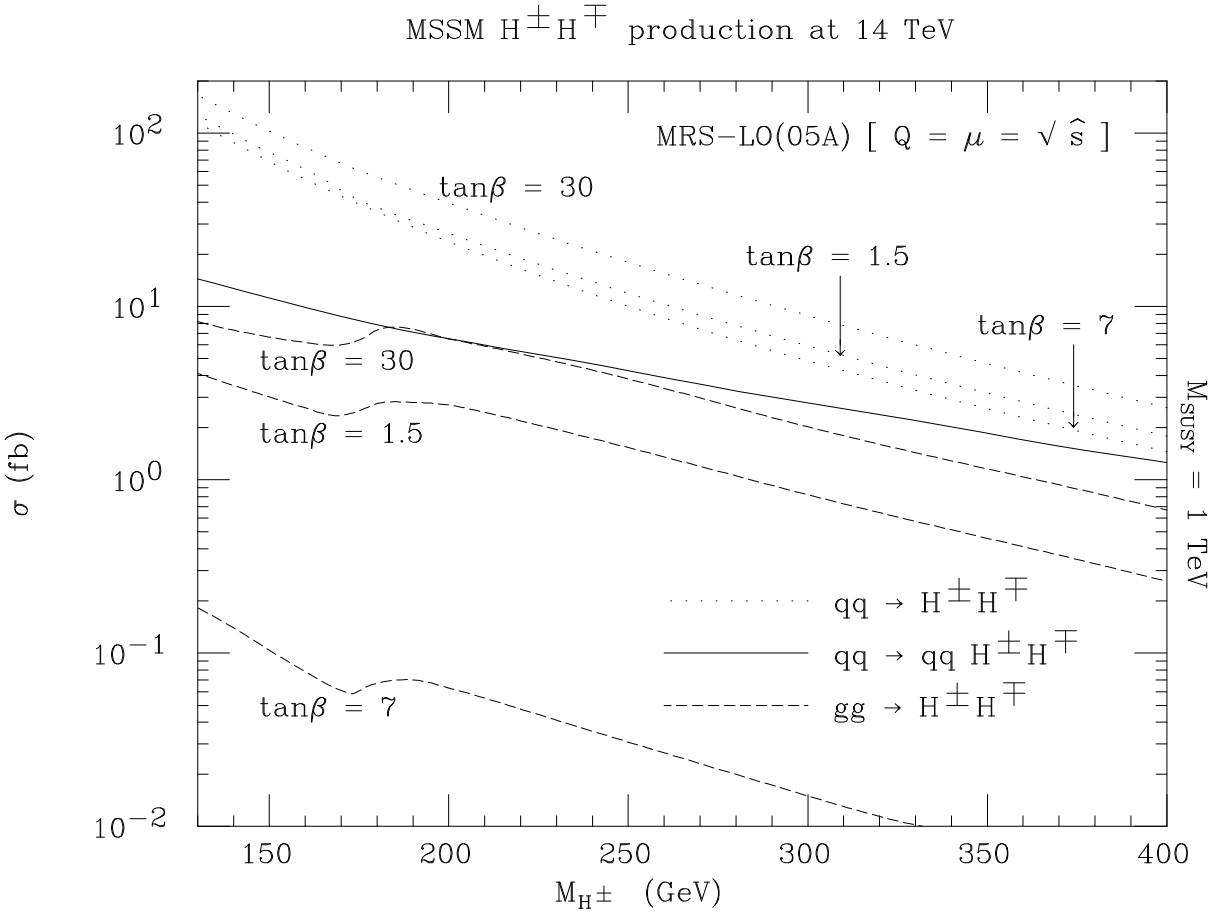

Figure 2: Cross section in femtobarns at the LHC for the following H^+H^- production processes discussed in the text: $q\bar{q} \to H^+H^-$ (including the $b\bar{b}$ contribution), $gg \to H^+H^-$ and $qq \to qqH^+H^-$, for $\tan\beta = 1.5, 7$ and 30. In the last process, there is no visible $\tan\beta$ dependence.

Diagrams by FEYNMAN DRAW

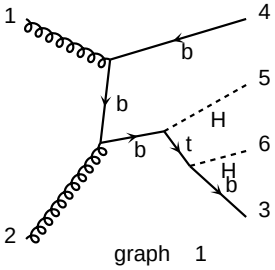

graph 1

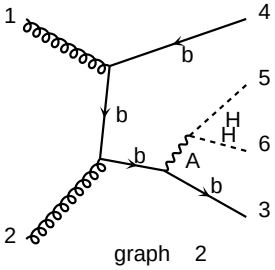

graph 2

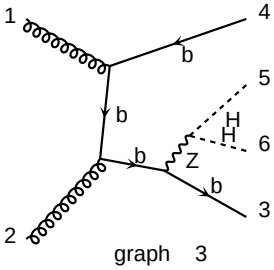

graph 3

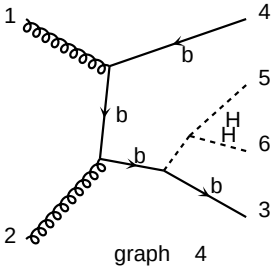

graph 4

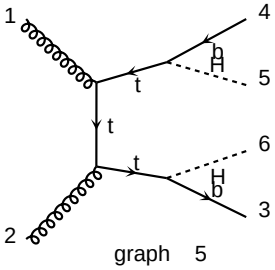

graph 5

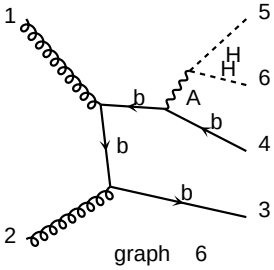

graph 6

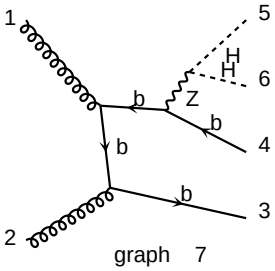

graph 7

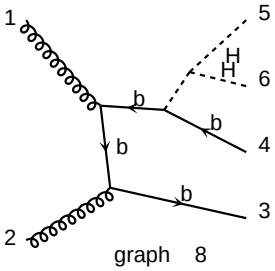

graph 8

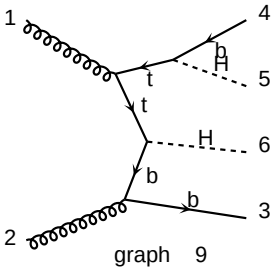

graph 9

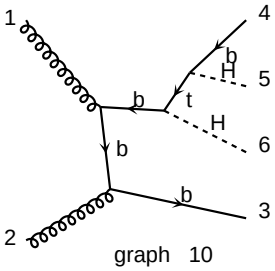

graph 10

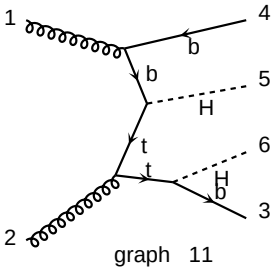

graph 11

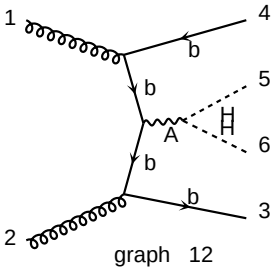

graph 12

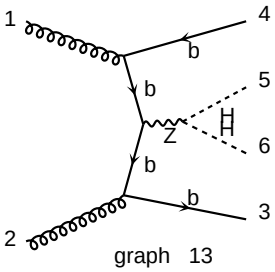

graph 13

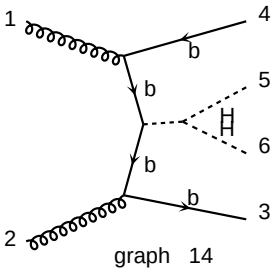

graph 14

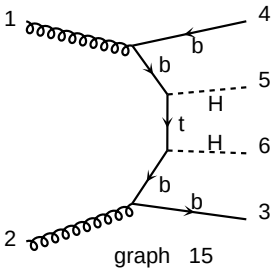

graph 15

continue

Diagrams by FEYNMAN DRAW

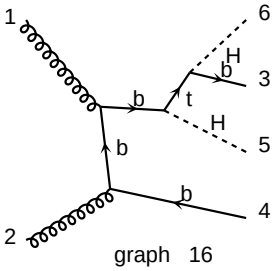

graph 16

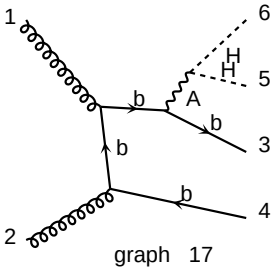

graph 17

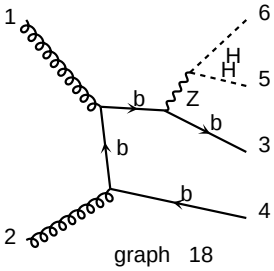

graph 18

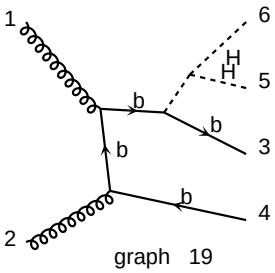

graph 19

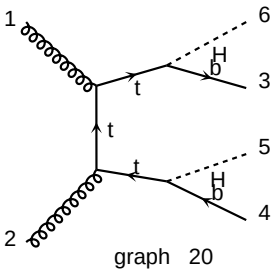

graph 20

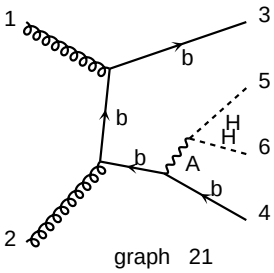

graph 21

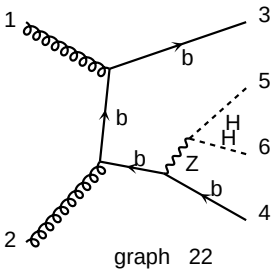

graph 22

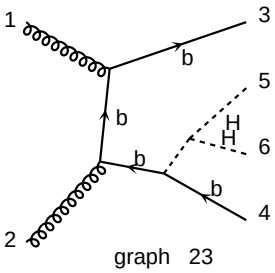

graph 23

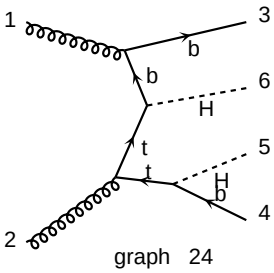

graph 24

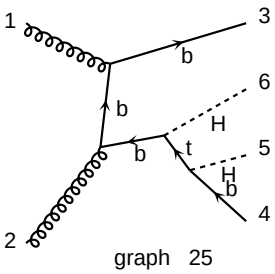

graph 25

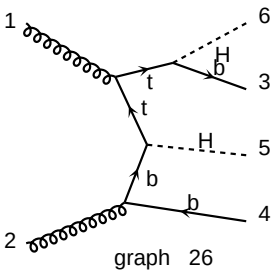

graph 26

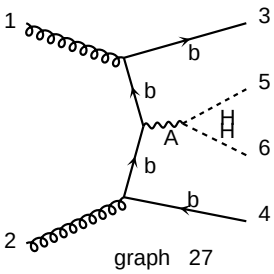

graph 27

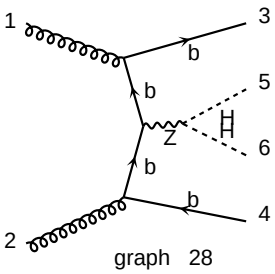

graph 28

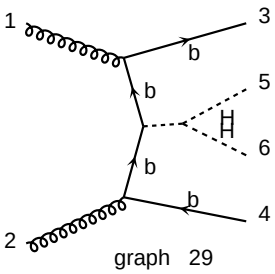

graph 29

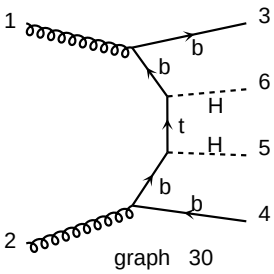

graph 30

continue

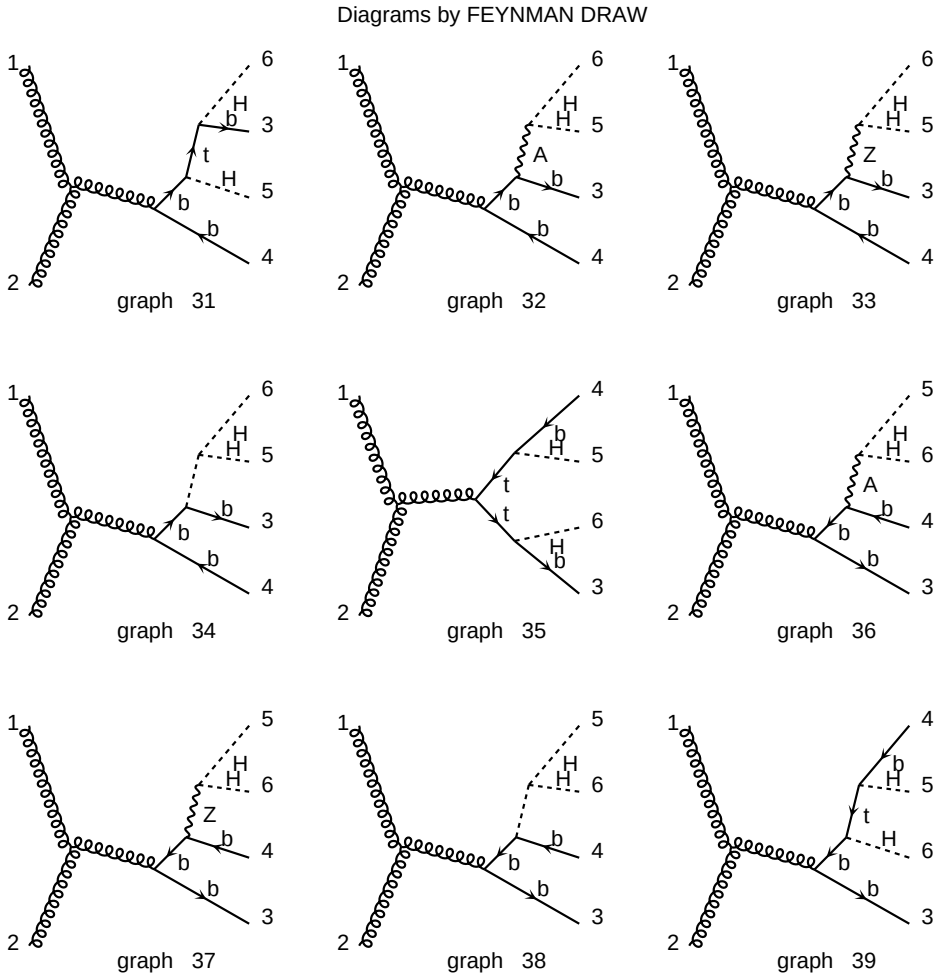

Figure 3: Feynman diagrams at tree level for process (2). The labels `b, t, A, Z, W and H` refer to a b, t-(anti)quark, γ, Z, $W^{\pm}$ and $H^{\pm}$ boson, respectively, whereas an unlabelled, (internal)[external] (dashed)[helical] line represents a (summation over H and h boson propagators)[gluon].

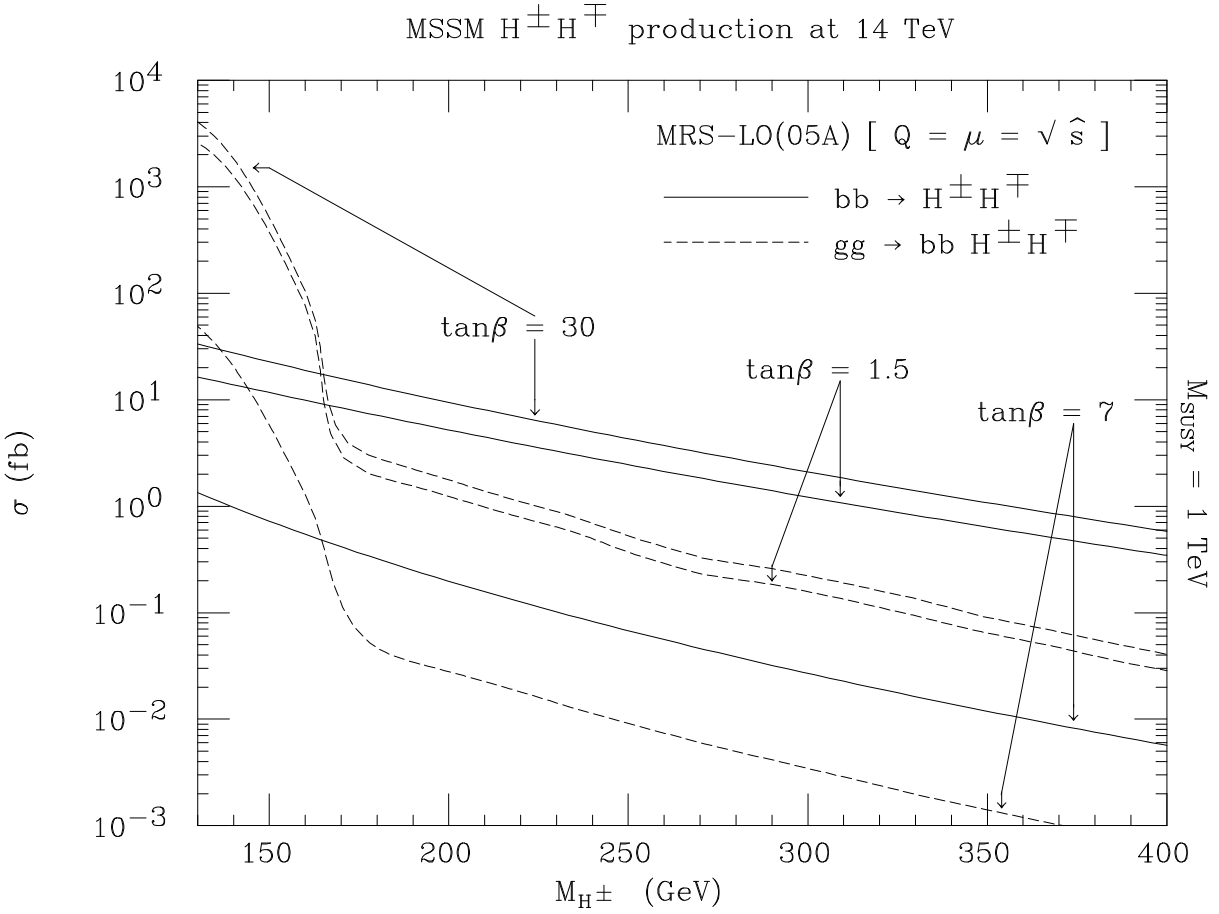

Figure 4: Cross section in femtobarns at the LHC for the following H^+H^- production processes discussed in the text: $b\bar{b} \to H^+H^-$ and $gg \to b\bar{b}H^+H^-$, for $\tan\beta = 1.5, 7$ and 30.

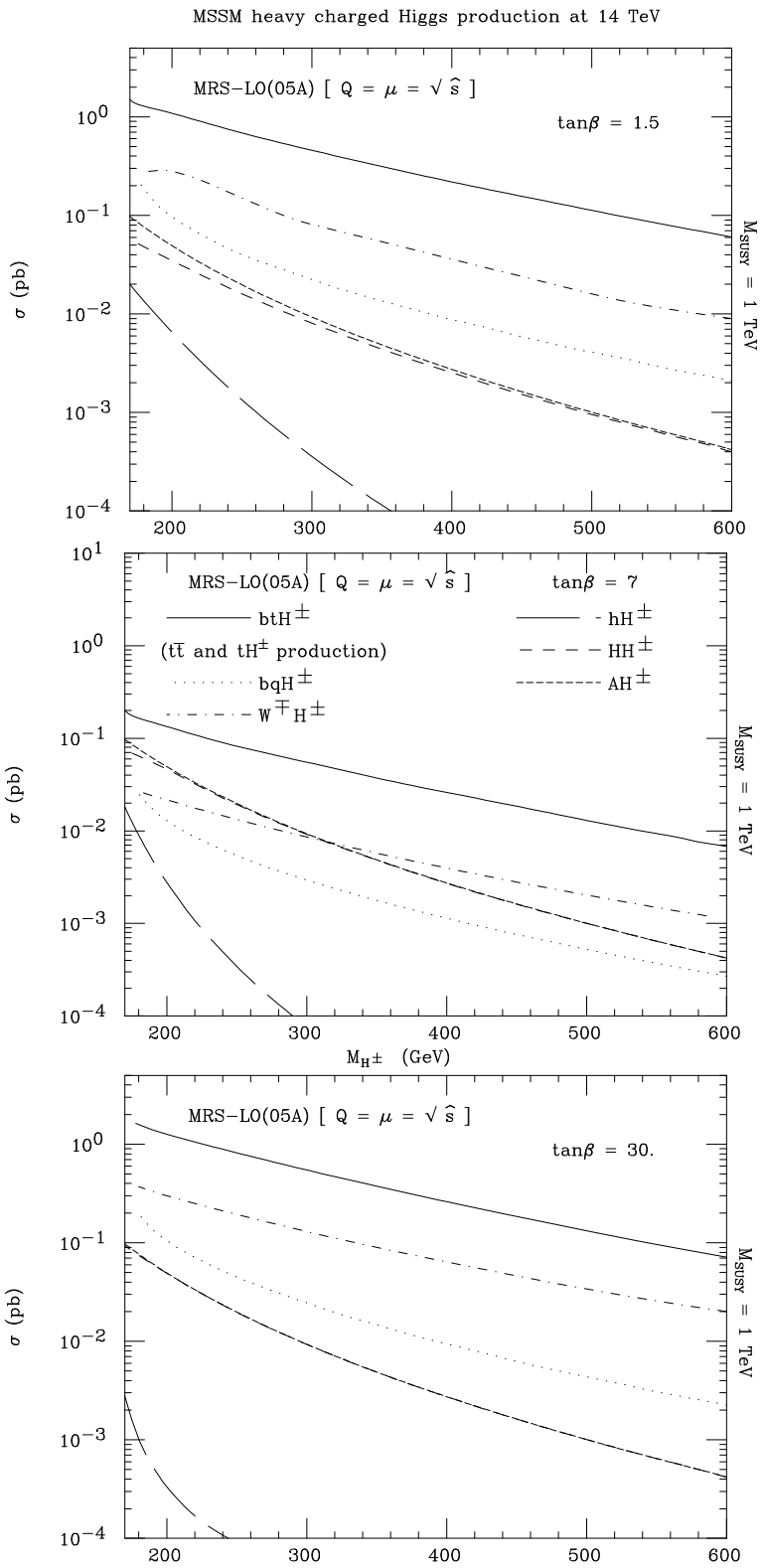

Figure 5: Cross sections in picobarns at the LHC for the production mechanisms of a single charged Higgs boson, for $\tan\beta = 1.5$ (top), 7 (middle) and 30 (bottom). (The $q\bar{q}' \to \Phi H^{\pm}$ rates, with $\Phi = h, A$, visually coincide for $\tan\beta = 30$.)

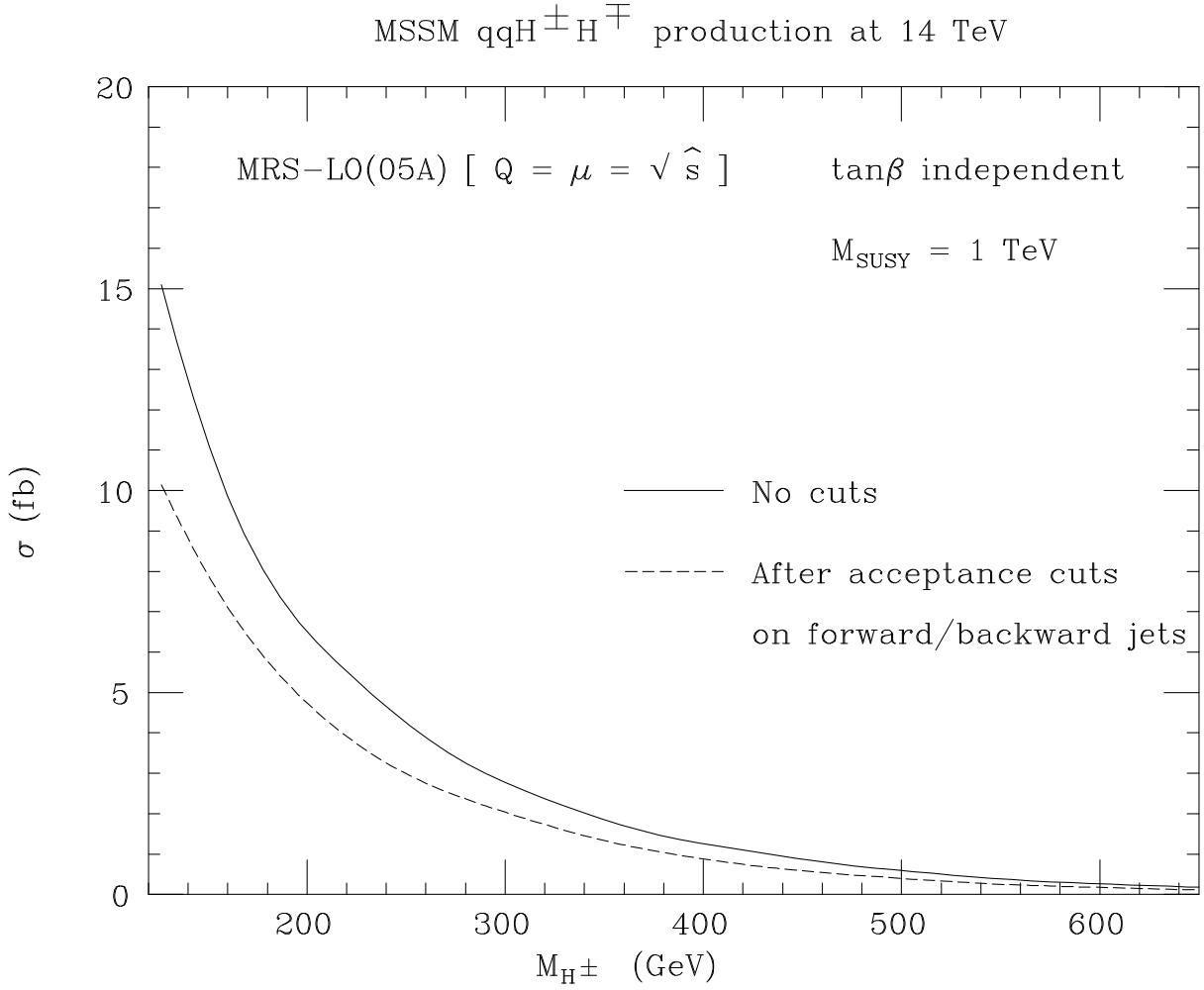

Figure 6: Cross sections in femtobarns at the LHC for process (1), without and with the following acceptance cuts on the forward jets: $p_T^j > 20$ GeV and $|\eta^j| < 5$. Here, there is no visible $\tan\beta$ dependence.

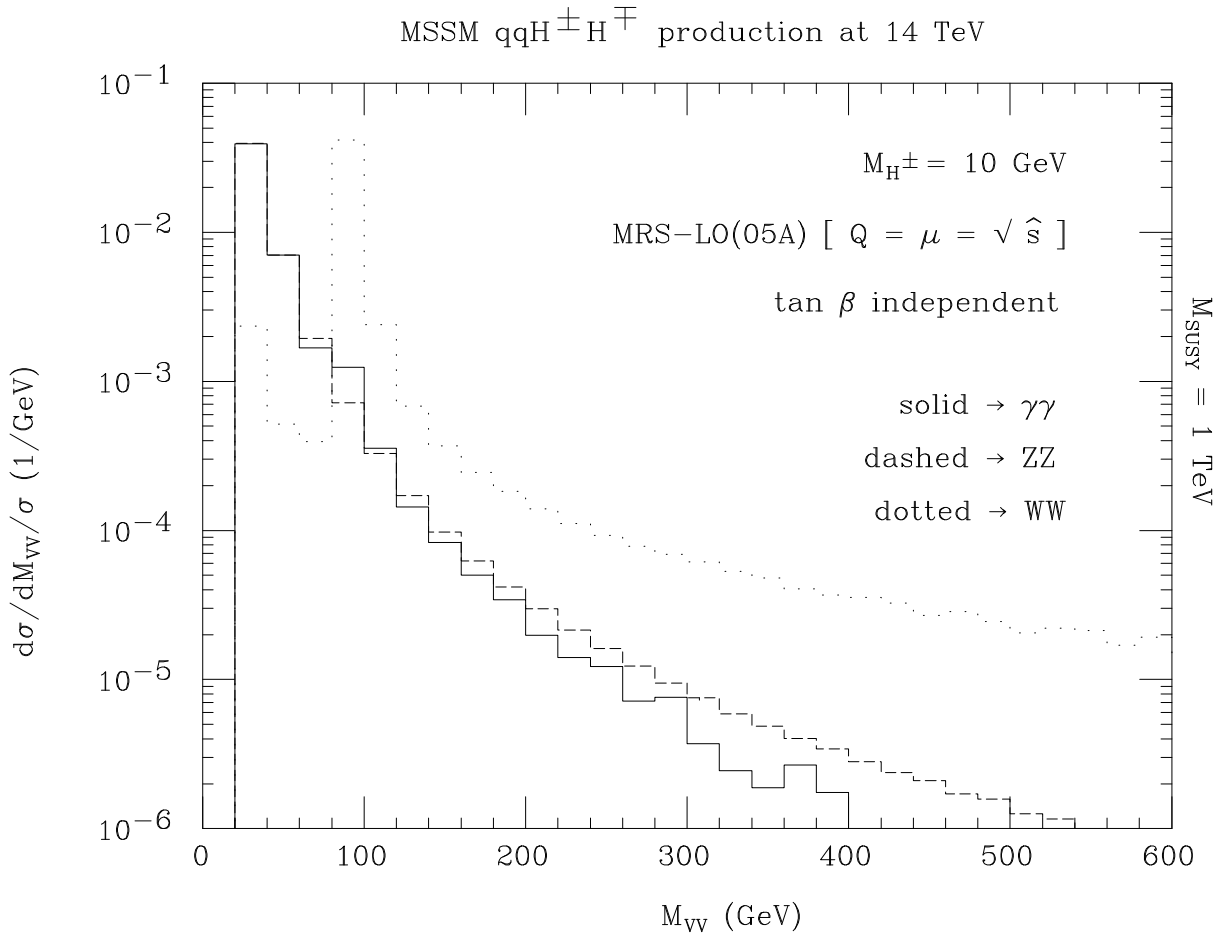

Figure 7: Mass distribution of the vector-vector system recoiling against the forward/backward jets, before any cuts, in case of the the $\gamma\gamma, ZZ$ and W^+W^- mediated graphs, out of the full set of process (1), for the 'illustrative' value $M_{H^\pm}$=10 GeV. Here, there is no visible $\tan\beta$ dependence.

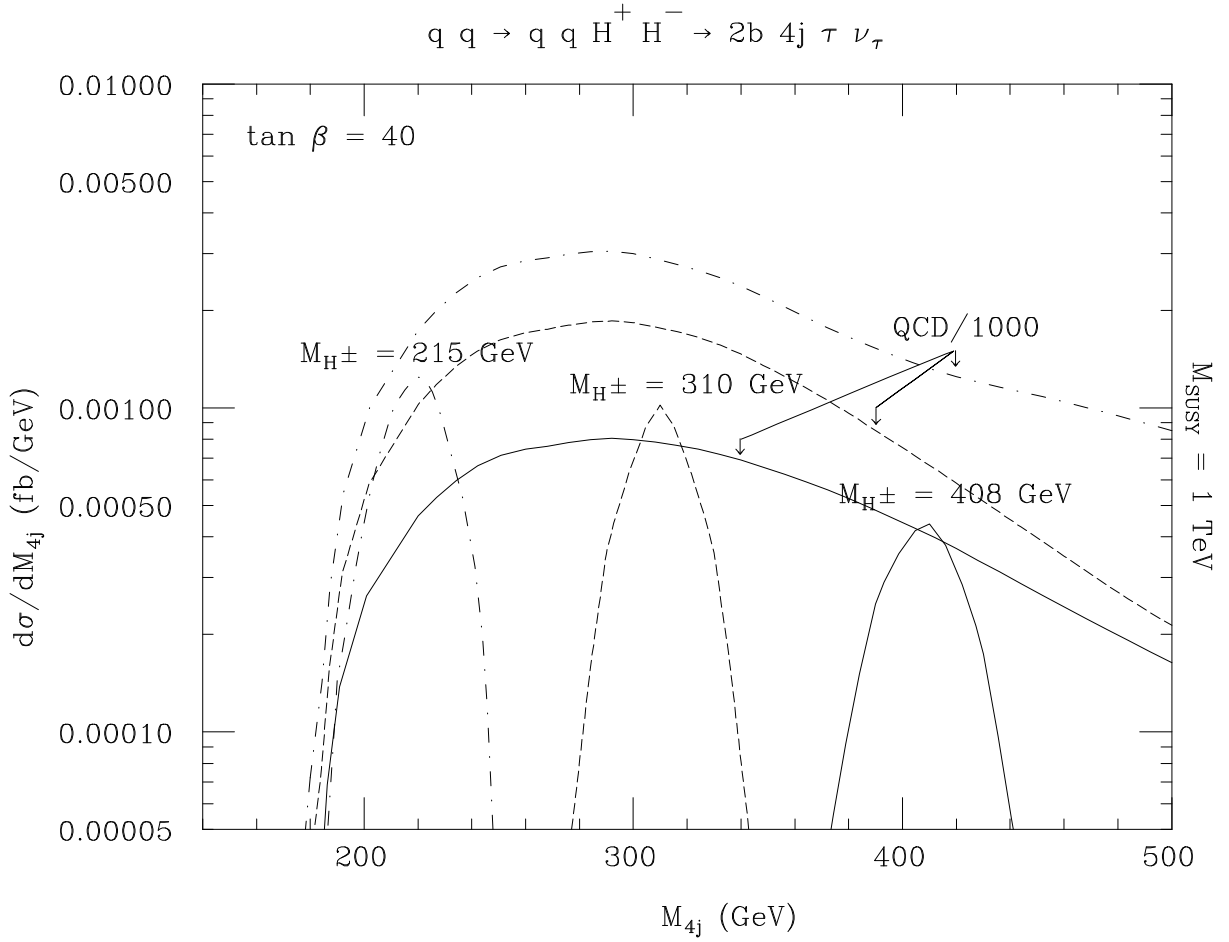

Figure 8: Mass distribution of the four-jet system recoiling against the $j_1 j_2$ and $\tau^{\pm}$-neutrino pairs, after the selection described in points 2.–8., in case of process (1) and of the QCD background $q\bar{q}, gg \to t\bar{t}gg$, for three choices of $M_{H^{\pm}}$ in the heavy mass range and $\tan\beta = 40$, in the channel '6 jets + $\tau^{\pm}$ + missing energy'.